Nonequilibrium isolated molecule limit

Michael Galperin,[1, *] Abraham Nitzan,[2] and Mark A. Ratner[3]

[1]*Department of Chemistry & Biochemistry, University of California San Diego, La Jolla, CA 92093-0340, USA*
[2]*School of Chemistry, The Sackler Faculty of Sciences, Tel Aviv University, Tel Aviv 69978, Israel*
[3]*Department of Chemistry and Materials Research Center,*
Northwestern University, Evanston IL 60208, USA
(Dated: August 22, 2008)

Method developed by Sandalov and coworkers [Int. J. Quant. Chem. **94**, 113 (2003)] is applied to inelastic transport in the case of strong correlations on the molecule, which is relatively weakly coupled to contacts. Ability of the approach to deal with the transport in the language of many-body molecular states as well as take into account charge-specific normal modes and nonadiabatic couplings is stressed. We demonstrate capabilities of the technique within simple model calculations, and compare it to previously published approaches.

I. INTRODUCTION

Development of experimental capabilities dealing with nanostructures brings necessity of appropriate theoretical description of quantum transport (charge, spin, and heat) in mesoscopic junctions to the forefront of research.[1] Indeed, a lot of work has been done in this direction. In particular, many approaches are based on the Landauer expression for current through such junctions in elastic tunneling regime.[2] One of specific features of molecular transport junctions, the focus of molecular electronics, is flexibility of the molecules, which results in inelastic features being much more pronounced in transport through such junctions as compared e.g. to semiconductor quantum dots. Inelastic features are used as a diagnostic tool, helping to assure presence of the molecule and study its characteristics in the junction within inelastic electron tunneling spectroscopy both in the off-resonance (IETS)[3] and resonant tunneling (RIETS)[4] situations. Detailed discussion of the inelastic transport in molecular junctions can be found in Refs. 5,6.

Theoretical description of IETS is well established today both within simple models[7,8,9,10,11,12] and more realistic calculations.[13,14,15,16,17,18] Ability to predict quantitatively experimental findings is a sign of maturity of the field. From theoretical perspective this success is caused by ability to use well-established nonequilibrium perturbation (in electron-vibration coupling) technique. Indeed, in the off-resonant situation electron-vibration coupling M is an effectively small parameter, $M \ll \sqrt{\Delta E^2 + (\Gamma/2)^2}$ with ΔE being resonant off-set and Γ characterizing strength of molecule-contacts coupling. This allows expansion of the evolution operator in powers of M, and truncation at low (M^2) order, the Born approximation, is usually sufficient to get quantitatively correct predictions of IETS signal in molecular junctions.

Resonant tunneling situation, $\Delta E = 0$, provides richer physics. While weak electron-vibration coupling, $M \ll \Gamma$, is treated within perturbation theory also here,[19,20] the last fails in the opposite situation, $M > \Gamma$, when e.g. formation of polaron on the molecule becomes pos-

sible. Theoretically this case till now mostly was treated either within scattering theory (or isolated molecule) approach,[21,22,23,24] or within quasiclassical (rate or generalized rate equations) scheme.[20,25,26] While the first treats electron-vibrational interaction (numerically) exactly, it disregards Fermi populations in the contacts, as well as dynamical features due to their presence,[27] and may lead to erroneous predictions.[20,28] The last disregards quantum correlations, and as such is applicable to either high temperature, $k_B T \gg \hbar\omega$, (truly classical) situations, or (for generalized rate equations approach) quantum situations when correlations in the system die much quicker than electron transfer (between contact and molecule) time ($\sim 1/\Gamma$). Besides, these schemes lack formal procedure for improvement of their results similar to taking into account higher order terms in perturbative expansion. Recently we proposed nonequilibrium equation-of-motion (EOM) approach perturbative in molecule-contact coupling capable of dealing with RIETS situation.[28] The approach is formulated for simple resonant level model, but can be easily generalized for more realistic situations.[29] While it incorporates contacts (and hence nonequilibrium character of the junction) into consideration, the price to pay is (generally) more approximate level of description of electron-vibration interaction on the bridge. Alternatively, schemes exploring particular parameter regions (slow vibration $\omega_0 < \Gamma$,[30,31,32] small, $V \ll \omega_0$,[33] or big, $V \gg \omega_0$,[34] bias) were proposed at a model level.

Another point especially important for resonant transport (both elastic and inelastic), when actual oxidation or reduction of the molecule takes place, is necessity to speak in the language of many-body molecular states contrary to single-particle molecular orbitals (the last is used in most ab initio transport calculations today). This includes electronic structure reorganization upon charging, state dependent vibrational modes, anharmonicities, and non-Born-Oppenheimer couplings. First schemes trying to treat transport in a many-body molecule states language were recently proposed.[25,26,35]

Difficulties in describing RIETS stem from absence of

well-established *nonequilibrium atomic limit* for molecule in the junction. Indeed, contacts play role of boundary conditions responsible for establishing nonequilibrium state of the molecule. The last is a complicated mixture of different charge (and excitation) states. Approaches developed in molecular electronics community so far either disregard boundary conditions and treat molecule as an equilibrium object (scattering theory and isolated molecule treatments), or establish this nonequilibrium state (mostly nonequilibrium Green function, NEGF, approaches) being unable to map it into separate charge (or more exactly state) constituents. Note, density matrix based schemes capable of such mapping were developed recently.[36,37] Such schemes however, miss time correlations, which may become important in e.g. noise spectrum calculations.

Hubbard operators is a natural language to talk about system (in our case subsystem - molecule) in terms of its states. Thus one seems to be interested in utilizing nonequilibrium Hubbard operator Green function technique for description of situations similar to RIETS, when ability to establish nonequilibrium atomic limit of system is desirable. The approach should be capable to provide a systematic way to take correlations into account (similar to perturbative expansion in standard diagrammatic techniques). Such approach originating from Kadanoff and Baym functional derivative EOM scheme, was developed in the form of equilibrium Hubbard operator GFs by Sandalov and coworkers for materials with strong electron correlations (magnets with localized and partly localized moments, Mott insulators, Kondo lattices, heavy fermion systems, and high-Tc superconductors).[38] The method so far has been applied to model elastic transport through quantum dots[39,40,41] and lowest states of double quantum dots,[42,43,44,45] and is completely ignored in the molecular electronics community.

The goal of our present consideration is to introduce inelastic transport description in the Coulomb blockade regime within proper non-equilibrium atomic limit, and to attract attention of the molecular electronics community to the proper nonequilibrium approach capable of speaking in the language of many-particle states (rather than single-particle orbitals) and taking into account both molecular charge state dependent normal modes (presently largely ignored in simulations) and non-adiabatic couplings. Note, that Kondo physics is beyond the scope of current consideration. The approach takes into account only on-the-molecule correlations in a way that generalizes previous considerations.[25,26] Note, that including many-body molecular states into consideration of transport potentially allows for: 1. Much more accurate molecular structure simulation out of equilibrium than in current ab initio schemes, due to possibility to employ equilibrium quantum chemistry methods as a starting point for self-consistent procedure. 2. Proper treatment of oxidation/reduction and corresponding electronic and vibrational molecular structure changes, as well as non-adiabatic couplings, 3. Ability to deal with general form of electron-vibration interaction as long as it is localized in space (in the spirit of Ref. 23 but in addition retaining many-body character of the junction), 4. Calculation of noise spectrum of the junction due to preserved time correlations (see e.g. Ref. 46 for detailed discussion), 5. Proper treatment of degenerate situations due to preserved space correlations (see e.g. Ref. 47 for discussion). Structure of the paper is the following. In Section II we briefly describe the method in terms of many-electronic states of the system, and compare it to previously proposed generalized master equation scheme. Section III presents numerical examples of its application to transport with discussion. Section IV concludes.

II. METHOD

Here we introduce model of molecular junction, briefly review the basics of nonequilibrium Hubbard Green function technique, and compare it to previously proposed generalized master equation approach.

A. Model

As usual we consider molecular junction consisting of 3 parts: left (L) and right (R) contacts and the molecule (M). The contacts are assumed to be reservoirs of free electrons each at its own equilibrium. Molecule (or supermolecule if inclusion of parts of contacts is required) is the nonequilibrium part of the system. Besides, any external potential, e.g. gate voltage probe, or additional contacts can be added to the picture if necessary. The Hamiltonian of the system is

$$\hat{H} = \hat{H}_L + \hat{H}_M + \hat{H}_R + \hat{H}_T \qquad (1)$$

where $\hat{H}_K$ $(K = L, R)$ is Hamiltonian for contact K

$$\hat{H}_K = \sum_{k \in K} \varepsilon_k \hat{c}_k^\dagger \hat{c}_k, \qquad (2)$$

$\hat{H}_M$ is Hamiltonian of the isolated molecule, and $\hat{H}_T$ is coupling between the subsystems

$$\hat{H}_T = \sum_{k \in \{L,R\}; m \in M} \left(V_{km} \hat{c}_k^\dagger \hat{d}_m + V_{mk} \hat{d}_m^\dagger \hat{c}_k \right) \qquad (3)$$

$\hat{d}^\dagger$ $(\hat{d})$ and $\hat{c}^\dagger$ $(\hat{c})$ are creation (annihilation) operators for electron on the molecule and in the contacts, respectively. Their indices m and k denote electronic state in some chosen single-particle basis, and incorporate all the necessary quantum indices (e.g. site and spin).

Now we want to consider molecular subsystem in the basis of *many-electron states* $|N, i>$, where N stands for molecular charge (number of electrons or excess electrons

on the molecule) and i numerates different (e.g. excitation) states within the same charge state block. Generally these states should not be orthonormal, and consequences of overlap between different molecular states (as well as overlap of molecular and contact states) were considered in several papers.[38,48] In what follows however we chose the states $|N, i>$ to be orthonormal

$$< N, i | N', i' > = \delta_{N,N'} \delta_{i,i'} \tag{4}$$

in order to keep notation as simple as possible. Hubbard operators are introduced as usual

$$\hat{X}_{(N,i;N',i')} \equiv |N, i><N', i'| \tag{5}$$

In terms of these many-electron states transfer Hamiltonian becomes

$$\hat{H}_T = \sum_{k \in \{L,R\}; \mathcal{M}} \left(V_{k\mathcal{M}} \hat{c}_k^\dagger \hat{X}_{\mathcal{M}} + V_{\bar{\mathcal{M}}k} \hat{X}_{\mathcal{M}}^\dagger \hat{c}_k \right) \tag{6}$$

where

$$\mathcal{M} \equiv (N, i; N+1, j) \tag{7}$$

denotes transition of the system from state $|N+1, j>$ to state $|N, i>$, while $\bar{\mathcal{M}} \equiv (N+1, j; N, i)$ stands for the backward transition. Transfer matrix element is

$$V_{k\mathcal{M}} \equiv \sum_{m \in M} V_{km} < N, i | \hat{d}_m | N+1, j > \tag{8}$$

and $V_{\bar{\mathcal{M}}k} = V_{k\mathcal{M}}^*$. Often many-electron states are chosen as eigenstates of isolated molecule, in this case

$$\hat{H}_M = \sum_{|N,i>} E_{N,i} X_{(N,i;N,i)} \tag{9}$$

with $E_{N,i}$ energies of the isolated molecule states.

B. Current expression

Following derivation by Meir and Wingreen[49,50] one gets usual expression for the current at interface $K = L, R$

$$I_K(t) = \frac{e}{\hbar} \int_{-\infty}^t dt_1 \, \text{Tr} \big[\\
\Sigma_K^<(t,t_1) \, G^>(t_1,t) + G^>(t,t_1) \, \Sigma_K^<(t_1,t) \tag{10} \\
- \Sigma_K^>(t,t_1) \, G^<(t_1,t) - G^<(t,t_1) \, \Sigma_K^>(t_1,t) \big]$$

which for steady-state situation simplifies to

$$I_K = \frac{e}{\hbar} \int_{-\infty}^{+\infty} \frac{dE}{2\pi} \, \text{Tr} \left[\Sigma_K^<(E) \, G^>(E) - \Sigma_K^>(E) \, G^<(E) \right] \tag{11}$$

The only difference from the standard NEGF expression is that $\text{Tr}[\ldots]$ in (10) and (11) goes not over single-electron basis, but over basis of *single-electron transitions* $\mathcal{M}$, Eq.(7), between many-particle states of the molecule.

Self-energies Σ_K in (10) and (11) are defined on the Keldysh contour as

$$[\Sigma_K(\tau, \tau')]_{\mathcal{M}\mathcal{M}'} \equiv \sum_{k \in K} V_{\bar{\mathcal{M}}k} \, g_k(\tau, \tau') \, V_{k\mathcal{M}'} \tag{12}$$

with

$$g_k(\tau, \tau') \equiv -i < T_c \, \hat{c}_k(\tau) \, \hat{c}_k^\dagger(\tau') > \tag{13}$$

GF for free electrons in the contacts. SEs projections are

$$[\Sigma_K^<(E)]_{\mathcal{M}\mathcal{M}'} = i\Gamma_{\mathcal{M}\mathcal{M}'}^K(E) f_K(E) \tag{14}$$

$$[\Sigma_K^>(E)]_{\mathcal{M}\mathcal{M}'} = -i\Gamma_{\mathcal{M}\mathcal{M}'}^K(E) [1 - f_K(E)] \tag{15}$$

where

$$\Gamma_{\mathcal{M}\mathcal{M}'}^K(E) \equiv \sum_{k \in K} V_{\bar{\mathcal{M}}k} \, V_{k\mathcal{M}'} \, \delta(E - \varepsilon_k) \tag{16}$$

and $f_K(E)$ is the Fermi distribution in contact K.

GFs in (10) and (11) are Hubbard operator GFs defined on the Keldysh contour as

$$G_{\mathcal{M}\mathcal{M}'}(\tau, \tau') \equiv -i < T_c \, \hat{X}_{\mathcal{M}}(\tau) \, \hat{X}_{\mathcal{M}'}^\dagger(\tau') > \tag{17}$$

Note, that operators in (13) and (17) are in Heisenberg representation. Note also, that $\mathcal{M}$ and $\mathcal{M}'$ in (17) may be (in principle) arbitrarily far away from one another in the charge space. GF (17) represents correlation between different single-electron molecular many-body state transitions due to coupling to the same bath (contacts). In practice however, it seems unreasonable to go beyond correlations between nearest charge space blocks.

In order to show connection of the present formalism to previously proposed generalized rate equation (master equation in the Fock space) approach, we have to realize that the last misses correlations both in space and time. So to reduce present GF description to the master equation in the Fock space, we need to make several simplifications:

1. *Diagonal approximation.* We have to stick to diagonal elements of GF only $G_{\mathcal{M}\mathcal{M}}$ with $\mathcal{M} = (N, i; N+1, j)$.

2. *Markov approximation.* We have to consider only GFs of equal times $G(t,t)$. In order to reduce GFs of different times entering (11) to equal times quantities we use approximation

$$G_{\mathcal{M}\mathcal{M}}(t - t') \approx \exp[i\Delta_{\mathcal{M}}^0(t' - t)] G_{\mathcal{M}\mathcal{M}}(t - t) \tag{18}$$

where

$$\Delta_{\mathcal{M}}^0 \equiv E_{N+1,j} - E_{N,i} \tag{19}$$

Now, noting that

$$iG_{\mathcal{M}\mathcal{M}}^>(t - t) = P_i^N \tag{20}$$

$$-iG_{\mathcal{M}\mathcal{M}}^<(t - t) = P_j^{N+1} \tag{21}$$

are probabilities to find molecule in state $|N, i>$ and $|N + 1, j>$ respectively, we get from (11)

$$I_K = \frac{e}{\hbar} \sum_{N;i,j} \left(\Gamma^K_{(N,i;N+1,j)} f_K(E_j^{N+1} - E_i^N) P_i^N \right. \quad (22)$$

$$\left. - \Gamma^K_{(N,i;N+1,j)} [1 - f_K(E_j^{N+1} - E_i^N)] P_j^{N+1} \right)$$

If now one restricts attention only to particular charge space block N_0 and its nearest neighbors, one gets Eqs. (6) and (7) of Ref. 25.

C.   General equation for GF

Now, when expression for the current is established, we need a procedure to calculate Hubbard operators GF (17). Note, that standard diagrammatic techniques are inapplicable here, due to lack of the Wick's theorem (since Hubbard operators are many-particle operators). An alternative to diagrammatic expansion in the form of functional derivative equation-of-motion technique was developed in Ref. 38. Here we briefly review steps needed to obtain EOM for GF we will use in our numerical simulations.

Following Ref. 38 we start by writing EOM for Hubbard operator $\hat{X}_{\mathcal{M}}(\tau)$, where $\mathcal{M} \equiv (N, i; N + 1, j)$. This leads to

$$\left[i \frac{\partial}{\partial \tau} - \Delta^0_{\mathcal{M}} \right] \hat{X}_{\mathcal{M}}(\tau) =$$
$$\sum_{k \in \{L, R\}; \ell} \left(-V_{k(N+1,j;N+2,\ell)} \hat{c}_k^\dagger(\tau) \hat{X}_{(N,i;N+2,\ell)}(\tau) \right.$$
$$- V_{k(N-1,\ell;N,i)} \hat{c}_k^\dagger(\tau) \hat{X}_{(N-1,\ell;N+1,j)}(\tau) \quad (23)$$
$$+ V_{(N+1,j;N,\ell)k} \hat{X}_{(N,i;N,\ell)}(\tau) \hat{c}_k(\tau)$$
$$\left. + V_{(N+1,\ell;N,i)k} \hat{X}_{(N+1,\ell;N+1,j)}(\tau) \hat{c}_k(\tau) \right)$$

In what follows we disregard first 2 terms on the right-hand-side, since they describe simultaneous transfer of 2 electrons between contact and molecule, which is beyond the scope of this consideration. It is clear that when writing EOM for GF (17) terms in the right-hand-side of (23) will produce correlation functions of the form

$$< T_c \hat{X}_\xi(\tau) \hat{c}_k(\tau) \hat{X}^\dagger_{\mathcal{M}'}(\tau') > \quad (24)$$

which can not be factorized into product of single-excitation GF (17) and contact single-electron GF (13) due to lack of the Wick's theorem.

In order to make this separation a trick with auxiliary fields $\mathcal{U}_\xi(\tau)$ is employed. We need to introduce additional disturbance potential

$$\hat{H}_{\mathcal{U}}(\tau) \equiv \sum_{N;i,j} \mathcal{U}_{(N,i;N,j)}(\tau) \hat{X}_{(N,i;N,j)}(\tau) \quad (25)$$

and corresponding generating functional

$$\hat{S}_{\mathcal{U}} \equiv \exp \left[-i \int_c d\tau \, \hat{H}_{\mathcal{U}}(\tau) \right] \quad (26)$$

Then defining GF of 2 arbitrary operators $\hat{A}$ and $\hat{B}$ in the presence of auxiliary fields $\mathcal{U}$

$$G_{AB}(\tau, \tau') \equiv -i < T_c \hat{A}(\tau) \hat{B}(\tau') >_{\mathcal{U}} \quad (27)$$

$$\equiv -i \frac{< T_c \hat{S}_{\mathcal{U}} \hat{A}(\tau) \hat{B}(\tau') >}{< T_c \hat{S}_{\mathcal{U}} >}$$

one easily can get the following identity

$$-i < T_c \hat{X}_\xi(\tau'') \hat{A}(\tau) \hat{B}(\tau') >_{\mathcal{U}} \quad (28)$$

$$= \left[< T_c \hat{X}_\xi(\tau'') >_{\mathcal{U}} + i \frac{\delta}{\delta \mathcal{U}_\xi(\tau'')} \right] G_{AB}(\tau, \tau')$$

Eq.(28) allows to express correlation function (24) in terms of single-excitation GF and its functional derivatives relative to auxiliary fields. Note, that putting (at the end) auxiliary fields to be zero turns (27) into a standard definition of GF.

So, introducing auxiliary fields as in Eqs. (25) and (26) and using expression (28), one gets general EOM for Hubbard operator GF (17) in the form

$$\left[i \frac{\partial}{\partial \tau} - \Delta^0_{\mathcal{M}} \right] G_{\mathcal{M}\mathcal{M}'}(\tau, \tau')$$

$$- \sum_{\ell} \left(\mathcal{U}_{(N+1,j;N+1,\ell)}(\tau) G_{(N,i;N+1,\ell)\mathcal{M}'}(\tau, \tau') \right.$$

$$\left. - \mathcal{U}_{(N,\ell;N,i)}(\tau) G_{(N,\ell;N+1,j)}(\tau, \tau') \right)$$

$$= \delta(\tau, \tau') P_{\mathcal{M}\mathcal{M}'}(\tau)$$

$$+ \sum_{\ell} \left(\left[< T_c \hat{X}_{(N,i;N,\ell)}(\tau) >_{\mathcal{U}} + i \frac{\delta}{\delta \mathcal{U}_{(N,i;N,\ell)}(\tau)} \right] \quad (29) \right.$$

$$\times \sum_{\mathcal{M}''} \int_c d\tau'' \, \Sigma_{(N,\ell;N+1,j)\mathcal{M}''}(\tau, \tau'') G_{\mathcal{M}''\mathcal{M}'}(\tau'', \tau')$$

$$+ \left[< T_c \hat{X}_{(N+1,\ell;N+1,j)}(\tau) >_{\mathcal{U}} + i \frac{\delta}{\delta \mathcal{U}_{(N+1,\ell;N+1,j)}(\tau)} \right]$$

$$\left. \times \sum_{\mathcal{M}''} \int_c d\tau'' \, \Sigma_{(N,i;N+1,\ell)\mathcal{M}''}(\tau, \tau'') G_{\mathcal{M}''\mathcal{M}'}(\tau'', \tau') \right)$$

where $\Delta^0_{\mathcal{M}}$ is defined in (19) and

$$P_{\mathcal{M}\mathcal{M}'} \equiv < T_c \hat{X}_{(N,i;N,i')}(\tau) + \hat{X}_{(N+1,j';N+1,j)}(\tau) >_{\mathcal{U}} \quad (30)$$

Eq.(29) is a general equation for Hubbard operator GF, representing an alternative to standard diagrammatic technique approaches. Role of expansion in small parameter here play functional derivatives in auxiliary fields. Level of approximation is defined by order of the derivative used in evaluation of GF. At the end of differentiations auxiliary fields are put to be zero, and resulting expression is equation for GF at particular level of approximation.

D.   First loop approximation

The simplest approximation, Hubbard I (HI), is obtained from (29) by keeping only diagonal averages, omit-

ting all functional derivatives, and $\mathcal{U} \to 0$

$$\left[i\frac{\partial}{\partial\tau} - \Delta^0_{\mathcal{M}}\right] G_{\mathcal{M}\mathcal{M}'}(\tau,\tau') = \delta(\tau,\tau')\,\delta_{\mathcal{M}\mathcal{M}'}\,P_{\mathcal{M}} \quad (31)$$
$$+ P_{\mathcal{M}} \sum_{\mathcal{M}''} \int_c d\tau'' \Sigma_{\mathcal{M}\mathcal{M}''}(\tau,\tau'')\,G_{\mathcal{M}''\mathcal{M}'}(\tau'',\tau')$$

Following most of the papers, employed the method so far,[39,40,41] in our consideration we go one step further - we take one functional derivative to get so called first loop approximation. Note, here we take derivative of the GF only, disregarding fluctuations of the spectral weight P. After performing the differentiation once more we keep only diagonal averages, omit all functional derivatives, and $\mathcal{U} \to 0$. Since the procedure was described in details in many papers (see e.g. Refs. 38,41), here we present only final result

$$\left[i\frac{\partial}{\partial\tau} - \Delta^0_{\mathcal{M}}\right] G_{\mathcal{M}\mathcal{M}'}(\tau,\tau') - i\sum_{\kappa,\ell}\sum_{\mathcal{M}''}\int_c d\tau''$$
$$\left[\Sigma_{(N,\kappa;N+1,j)\mathcal{M}''}(\tau,\tau'')\,D_{\mathcal{M}''(N-1,\ell;N,i)}(\tau'',\tau+) \right.$$
$$\times\, G_{(N-1,\ell;N,\kappa)\mathcal{M}'}(\tau,\tau')$$
$$-\,\Sigma_{(N,\kappa;N+1,j)\mathcal{M}''}(\tau,\tau'')\,D_{\mathcal{M}''(N,\kappa;N+1,\ell)}(\tau'',\tau+)$$
$$\times\, G_{(N,i;N+1,\ell)\mathcal{M}'}(\tau,\tau')$$
$$+\,\Sigma_{(N,i;N+1,\kappa)\mathcal{M}''}(\tau,\tau'')\,D_{\mathcal{M}''(N,\ell;N+1,\kappa)}(\tau'',\tau+)$$
$$\times\, G_{(N,\ell;N+1,j)\mathcal{M}'}(\tau,\tau') \quad\quad (32)$$
$$-\,\Sigma_{(N,i;N+1,\kappa)\mathcal{M}''}(\tau,\tau'')\,D_{\mathcal{M}''(N+1,j;N+2,\ell)}(\tau'',\tau+)$$
$$\left. \times\, G_{(N+1,\kappa;N+2,\ell)\mathcal{M}'}(\tau,\tau')\right]$$
$$= \delta(\tau,\tau')\,\delta_{\mathcal{M}\mathcal{M}'}\,P_{\mathcal{M}}$$
$$+ P_{\mathcal{M}}\sum_{\mathcal{M}''}\int_c d\tau'' \Sigma_{\mathcal{M}\mathcal{M}''}(\tau,\tau'')\,G_{\mathcal{M}''\mathcal{M}'}(\tau'',\tau')$$

where $\mathcal{M} \equiv (N,i;N+1,j)$ and D is so called full locator, which (in the first loop approximation) obeys the same equation (32) as GF but without spectral weight $P_{\mathcal{M}}$ multiplying delta function in the right-hand-side.

Expressions for GFs G and D (first loop approximation) in the shorthand (matrix in both Fock space and Keldysh contour variables) notation can be written as

$$\hat{D}^{-1}\,G = P \quad\quad (33)$$
$$\hat{D}^{-1}\,D = 1 \qu\quad (34)$$

where

$$\hat{D}^{-1} \equiv \left[i\frac{\partial}{\partial\tau} - \Delta_{\mathcal{M}} - P\,\Sigma\right] \qu\quad (35)$$
$$\Delta_{\mathcal{M}} = \Delta^0_{\mathcal{M}} + \delta\Delta_{\mathcal{M}} \qu\quad (36)$$

and $\delta\Delta_{\mathcal{M}}$ is given by the second term in the left-hand-side of Eq.(32), it is responsible for shifts of transition energies in the molecule due to contacts induced correlation. One sees that Eq.(34) has usual structure of the Dyson equation, which is obtained in standard diagrammatic expansion. The only difference is dressing of SE Σ

by spectral weight P. Thus formally one can use all the standard equations, using dressed SE Σ everywhere, to get desired projections of GF D. When D is known, G is obtained by simple matrix multiplication

$$G = D\,P \qu\quad (37)$$

Note, side of matrix dressing by spectral weight P is different for Σ and G, compare Eqs. (35) and (37). Note also, that the scheme is self-consistent, since both transition energies shift $\delta\Delta$ and spectral weights P depend on GF G, while the last depends on these quantities. In particular ($\mathcal{M} \equiv (N,i;N+1,j)$)

$$P_{\mathcal{M}} = N_{N,i} + N_{N+1,j} \qu\quad (38)$$
$$N_{N,i} \equiv <\hat{X}_{(N,i;N,i)}> = iG^>_{\mathcal{M}\mathcal{M}}(t,t) \quad \text{for any j} \qu\quad (39)$$
$$N_{N+1,j} \equiv <\hat{X}_{(N+1,j;N+1,j)}> = -iG^<_{\mathcal{M}\mathcal{M}}(t,t) \quad \text{for any i} \qu\quad (40)$$

Here $N_{N,i}$ and $N_{N+1,j}$ are probabilities to find system in the state $|N,i>$ and $|N+1,j>$ respectively.

III. NUMERICAL RESULTS AND DISCUSSION

Here we present results of simulations within first loop approximation. In order to speed up calculations we employed also diagonal approximation.[60] We consider transport through quantum dot and double quantum dot, discuss obtained data, and compare it to previously published results.

A. Quantum dot

In the case of quantum dot molecular Hamiltonian is

$$\hat{H}_M = \sum_{\sigma=\{\uparrow,\downarrow\}} \varepsilon_\sigma\hat{n}_\sigma + U\hat{n}_\uparrow\hat{n}_\downarrow \qu\quad (41)$$

where σ indicates spin projection and $\hat{n}_\sigma = \hat{d}^\dagger_\sigma\hat{d}_\sigma$. Full Fock space of the molecular part of the system (without vibrations) consists of one empty state ($|0> \equiv |0,0>$), two single-electron states, ($|\uparrow> \equiv |1,\uparrow>$ and $|\downarrow> \equiv |1,\downarrow>$), and one doubly occupied state ($|2> \equiv |2,0>$). Transitions between these states to be considered are spin up electron transfers ($0\uparrow$ and $\downarrow 2$) and spin down electron transfers ($0\downarrow$ and $\uparrow 2$). Writing Eq.(32) in the basis of these transitions one gets equations obtained in Ref. 40.

Figure 1 presents conductance map for elastic transport through quantum dot. Parameters of the calculation are $T = 10$ K, $\varepsilon_\sigma = -0.5$ eV, $\Gamma^K_\sigma = 0.01$ eV ($\sigma = \uparrow,\downarrow$ and $K = L,R$), and $U = 1$ eV. As usually one has areas of blockaded transport (inside part of diamonds) with fixed population on the dot (0, 1, and 2 from right to left), and transition areas (between the diamonds) where population on the dot is noninteger (see e.g. Ref. 51 for more detailed discussion).
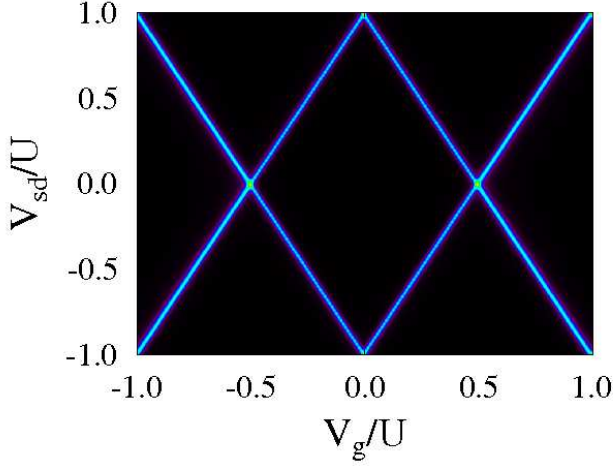
FIG. 1: (Color online) Conductance map for elastic transport through quantum dot. See text for parameters.

In order to treat inelastic transport we add to $\hat{H}_M$ molecular vibration linearly coupled to electron(s) on the dot

$$\omega_0 \hat{a}^\dagger \hat{a} + M(\hat{a} + \hat{a}^\dagger) \sum_\sigma \hat{n}_\sigma \qquad (42)$$

Such model is frequently used to describe inelastic transport in molecular junctions. In a sense it is similar to Marcus theory, and describes shift of the molecular vibration when molecule is charged due to electron transfer from/to the contacts. In general, model with non-diagonal electron-vibration coupling also can be considered within the formalism.

After small polaron (Lang-Firsov or canonical) transformation[52] linear coupling term is eliminated, while energy level position ε_σ and Hubbard repulsion U are renormalized ($\varepsilon_\sigma \to \varepsilon_\sigma - M^2/\omega_0$ and $U \to U - 2M^2/\omega_0$), and transfer matrix elements in $\hat{H}_T$, Eq.(3), are dressed with shift operators ($\hat{d}_\sigma \to \hat{d}_\sigma \hat{\mathcal{X}}$)

$$\hat{\mathcal{X}} = \exp\left[-\lambda(\hat{a}^\dagger - \hat{a})\right] \qquad (43)$$

where $\lambda = M/\omega_0$. In what follows we disregard renormalization of ε_σ and U, assuming that it was included in definition of these parameters.

Now molecule is characterized by direct product of electronic and vibrational spaces, so its state should be indicated by additional index v showing state of the vibration, i.e. molecular subspace is spanned by states $|0, v>$, $| \uparrow, v>$, $| \downarrow, v>$, and $|2, v>$, where $v \in \{0, 1, 2, 3, \ldots\}$. One has to consider the same electronic transitions as in the case of elastic transport, but in addition all possible transitions between states of the vibration have to be included. Transitions between these states (within the model) are possible only by electron transfer between molecule and contacts. Due to shift operators (43) appearing in $\hat{H}_T$ SEs (12) are now

dressed with corresponding vibrational overlap integrals ($\mathcal{M} \equiv (N, i, v_i; N+1, j, v_j)$)

$$\Sigma_{\mathcal{M}\mathcal{M}'} \to \Sigma_{\mathcal{M}\mathcal{M}'} \times <v_i|\hat{\mathcal{X}}|v_j> <v_i'|\hat{\mathcal{X}}|v_j'> \qquad (44)$$

with

$$<v|\hat{\mathcal{X}}|v'> = e^{-\lambda^2/2}(-1)^{(v-v')\theta(v-v')}\lambda^{v_{max}-v_{min}} \qquad (45)$$

$$\times \left[\frac{v_{min}!}{v_{max}!}\right]^{1/2} L_{v_{min}}^{v_{max}-v_{min}}(\lambda^2)$$

where v_{min} (v_{max}) is minimal (maximal) of v and v', $\theta(x)$ is step function, and L_n^m is Laguerre polynomial. Note an important formal difference between the present approach and the one presented in Ref. 51. While in the last we had to consider separately electron and phonon dynamics, which leads to convolution of electron GF (electron dynamics) with Franck-Condon factors (phonon dynamics), here the situation is different. Since we consider generalized Fock space (product of electronic and vibrational ones), within the formalism strictly speaking we do not have inelastic processes at all. Instead one has to consider elastic scattering events between electron-vibrational states. As a result the role played previously by the Franck-Condon factors (to introduce vibrational dynamics) now is included into Hubbard GF of the generalized Fock space.
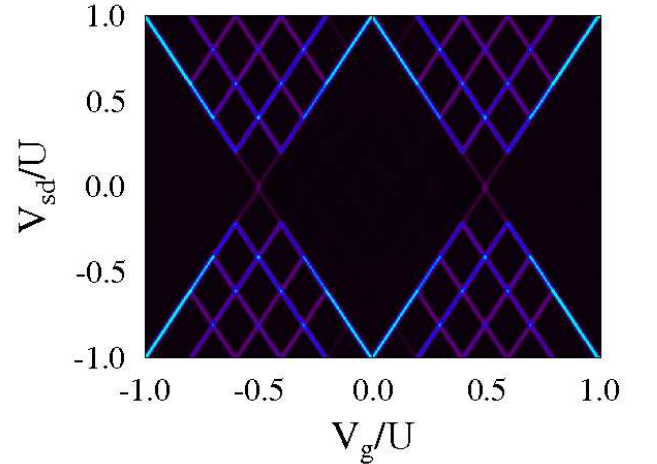

FIG. 2: (Color online) Conductance map for inelastic transport through quantum dot. Linear coupling model (42). See text for parameters.

Figure 2 presents conductance map for inelastic transport through quantum dot within linear coupling model (42). Parameters of the calculation are $\omega_0 = 0.2$ eV and $M = 0.4$ eV, all the other parameters are as in Fig. 1. Within the calculation we restricted vibrational subspace to 4 lowest levels ($v \in \{0, 1, 2, 3\}$). As expected, besides elastic peaks in the conductance map we get additional resonant vibrational features corresponding to inelastic processes. This Figure is equivalent to

Fig. 3a of Ref. 51, where calculation was done within perturbative (in coupling to electrodes) nonequilibrium EOM approach for the same model. As previously,[51] within the model (see also discussion below) distance between the diamond edges (elastic peak) and vibrational sidebands is defined by the oscillator frequency. Increase in electron-vibrational coupling would result in both more pronounced vibrational features and suppression of transport in the low source-drain voltage region due to Franck-Condon blockade. While increase in temperature would produce also vibrational sidebands corresponding to phonon absorption (features inside the diamond).

Finally, we want to demonstrate capabilities of the present scheme, which go beyond approaches previously used to treat inelastic transport. Suppose our molecule is small enough, so that upon charging it changes its normal modes essentially. Suppose also, that from all the normal modes of the molecule only one is coupled to tunneling electron. Inelastic transport in this case can be modeled by assigning different vibration frequencies to different charge states of the molecule. In our quantum dot model this corresponds to situation, when vibrational frequencies for $|0, v>$, $|\sigma, v>$, and $|2, v>$ states are different - $\omega_0^{(0)}$, $\omega_0^{(1)}$, and $\omega_0^{(2)}$ respectively. Self-energies due to electron transfer between molecule and contacts once more have to be dressed by overlap integrals between different vibrational wavefunctions, as is shown in Eq.(44). However this time (when vibrational frequencies change) the integrals should be calculated in the way discussed in Refs. 53,54
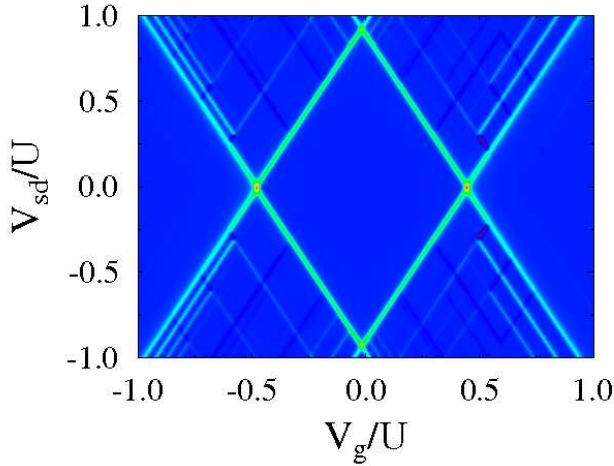

FIG. 3: (Color online) Conductance map for inelastic transport through quantum dot. Charge state dependent frequencies. See text for parameters.

Figure 3 presents conductance map for inelastic transport through quantum dot, when vibrational frequency depends on charge state of the dot. Parameters of the calculation are $\omega_0^{(0)} = 0.2$ eV, $\omega_0^{(1)} = 0.3$ eV, $\omega_0^{(2)} = 0.25$ eV and shift vector for both transitions was taken to be

0.5 Å(see Refs. 53,54 for detailed explanation), all the other parameters are as in Fig. 1 One sees that result of calculation is counter intuitive at the first sight. Naively one could expect to see inelastic peaks at each diamond edge (each charge state of the quantum dot) being separated by frequency corresponding to the neighboring charge state (RIETS probes frequencies of the intermediate ion). Real picture is more complicated however. Let consider electron transfer between 2 particular charge states of the quantum dot, say between states $|0, v_0 >$ and $|\sigma, v_1 >$ upon electron transfer from contact to molecule. In this case change in the subsystem energy, which will be observed in transport as inelastic peak in conductance, is $v_1\omega_0^{(1)} - v_0\omega_0^{(0)}$ (we omit here change in elastic electronic energy for simplicity, this will define only position of the elastic peak in conductance). Since v_0 and v_1 in principle can be any non-negative numbers, it is clear that one can observe a a progression of frequencies. Note, that in this progression one can see inelastic peaks in conductance, separated from the elastic one by frequency which does not exist in the system at all (e.g. $\omega_0^{(1)} - \omega_0^{(0)}$). Note also, that due to overlap factors involved the lowest frequencies of the progression will be observed better in RIETS signal. Non-adiabatic couplings can be included in calculation in a similar way.

B. Double quantum dot

Molecular Hamiltonian for double quantum dot is

$$\hat{H}_M = \sum_{i=\{1,2\} \, \sigma=\{\uparrow,\downarrow\}} \varepsilon_{i\sigma}\hat{n}_{i\sigma} - t_{12,\sigma}\left(\hat{d}_{1\sigma}^\dagger\hat{d}_{2\sigma} + \hat{d}_{2\sigma}^\dagger\hat{d}_{1\sigma}\right)$$

$$+ \sum_i U_i\hat{n}_{i\uparrow}\hat{n}_{i\downarrow} + U_{12}\hat{n}_1\hat{n}_2 \qquad (46)$$

where $i = \{1,2\}$ numbers sites and $\sigma = \{\uparrow, \downarrow\}$ stands for spin projection, $\hat{d}^\dagger$ $(\hat{d})$ is creation (annihilation) operator, $\hat{n}_{i\sigma} = \hat{d}_{i\sigma}^\dagger\hat{d}_{i\sigma}$, and $\hat{n}_i = \hat{n}_{i\uparrow} + \hat{n}_{i\downarrow}$. We assume that site 1 is coupled to the left contact, while site 2 - to the right.

We chose many-body states for molecular subsystem in the form $|1 \uparrow, 1 \downarrow, 2 \uparrow, 2 \downarrow>$. Unlike choice of Refs. 42,43,44,45 these are not eigenstates of the molecular Hamiltonian. As a result EOM for Hubbard operator GFs couples them also by hopping $t_{12,\sigma}$. Besides this all the treatment presented in Section II remains the same. There are 16 states (1, 4, 6, 4, and 1 states for 0, 1, 2, 3, and 4 electrons in the system respectively) and 32 single-electron transitions (16 for each spin block) to be considered.

Figure 4 shows conductance map for elastic transport through double quantum dot. Parameters of the calculation are $T = 10$ K, $\varepsilon_{i\sigma} = -0.5$ eV, $t_{12,\sigma} = 0.01$ eV, $\Gamma_{1\sigma}^L = \Gamma_{2\sigma}^R = 0.01$ eV, $\Gamma_{1\sigma}^R = \Gamma_{2\sigma}^L = 0$, $U_1 = U_2 = U = 1$ eV, $U_{12} = 0.5$ eV, and $E_F = 0.5$ eV. As usually one sees pattern of blockaded and allowed transport regions.
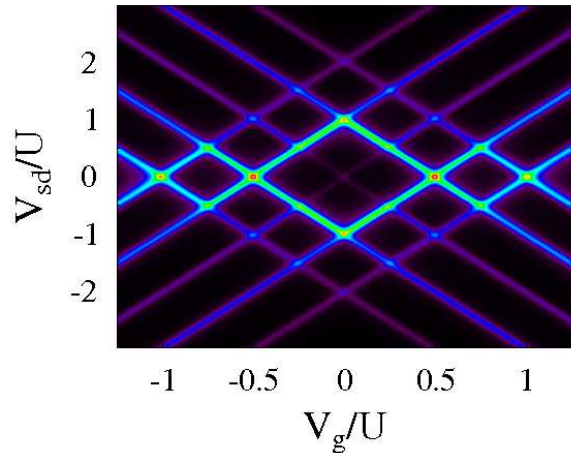
FIG. 4: (Color online) Conductance map for elastic transport through double quantum dot. See text for parameters.

However, here this pattern is more complicated than in the case of quantum dot. Figure 5 demonstrates this pattern for a horizontal cut of Fig. 4 at source-drain voltage $V_{sd}/U = 0.25$. Shown are current (a) and probabilities to find the molecular subsystem in different occupation states.
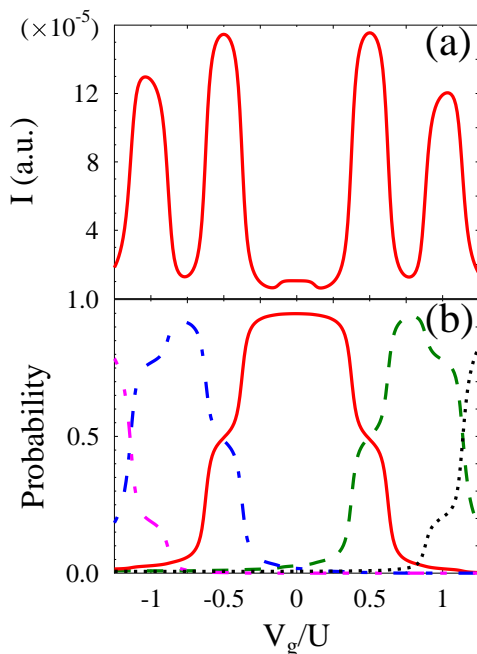

FIG. 5: (Color online) Elastic transport quantum dot at fixed source-drain voltage $V_{sd}/U = 0.25$: (a) Current vs. gate voltage, (b) Probability to find double quantum dot empty (dotted line, black), singly- (dashed line, green), doubly- (solid line, red), triply- (dash-dotted line, blue), or fully-occupied (dash-double-dotted line, magenta). Parameters are the same as in Fig. 4.

IV.   CONCLUSION

Approaches based on renormalization group technique (NRG, DMRG, real time RG, etc.) are routinely used to treat quantum impurity systems, where e.g. correlations between localized impurity (quantum dot or molecule) and delocalized states (contacts) leads to Kondo effect. Mostly these approaches were applied to description of strongly correlated systems in equilibrium. Description of transport is more problematic, since one needs to know spectral function at finite temperature, where all excitations may contribute.[55] Nevertheless first approaches dealing with transport started to appear as well.[36,55,56,57,58,59] The main complication with implementation of these methods (besides DMRG) for ab initio calculation is their complexity, so that all the calculations done so far are restricted to simple models only. In the case of molecular junctions most of ab initio calculations done today are performed at the mean mean field level of treatment with effective single particle orbitals used in place of molecular states. Such approach clearly breaks down in the resonance tunneling regime, where actual reduction/oxidation of the molecule leading to corresponding electronic and vibrational structure change become possible. Necessity of treating this regime in the language of many-body molecular states, thus incorporating on-the-molecule correlations, was realized and first approaches like e.g. generalized master equation approach[25,26] where proposed. Here we generalize this consideration by incorporating many-body molecular states language into nonequilibrium Green's function framework. The main formal problem here is that many-body states language makes the Wick's theorem inapplicable, and thus standard nonequilibrium diagrammatic techniques can not be used. A workaround based on functional derivative equation-of-motion technique for Hubbard operator GFs was developed by Sandalov and coworkers[38] for equilibrium case. The method so far has been applied to model elastic transport through quantum dots[39,40,41] and lowest states of double quantum dots,[42,43,44,45] and is completely ignored in the molecular electronics community. Here we employ the approach to deal with inelastic transport through molecular junctions in nonequilibrium atomic limit. We formulate the method within basis of charged states of the molecule. We demonstrate its ability to deal with transport situation in the language of these states (rather than effective single-electron orbitals), as well as take into account charge-specific normal modes as well as nonadiabatic couplings. Capabilities of the technique are illustrated with simple model calculations of transport through quantum dot and double quantum dot. Extension to realistic calculations is the goal of our future research.

Acknowledgments

[*] Previous address: Theoretical Division and Center for Integrated Nanotechnologies, Los Alamos National Laboratory, Los Alamos NM 87545, USA

[1] A.Nitzan and M.A.Ratner, Science **300**, 1384 (2003).

[2] R.Landauer, IBM J. Res. Dev. **1**, 223 (1957).

[3] B.C.Stipe, M.A.Rezaei, and W.Ho, Phys. Rev. Lett. **82**, 1724 (1999).

[4] N.B.Zhitenev, H.Meng, and Z.Bao, Phys. Rev. Lett. **88**, 226801 (2002).

[5] M.Galperin, M.A.Ratner, and A.Nitzan, J. Phys.: Condens. Matter **19**, 103201 (2007).

[6] M.Galperin, M.A.Ratner, A.Nitzan, and A.Troisi, Science **319**, 1056 (2008).

[7] R.Lake and S.Datta, Phys. Rev. B **45**, 6670 (1992).

[8] R.Lake and S.Datta, Phys. Rev. B **46**, 4757 (1992).

[9] S.Tikhodeev, M.Natario, K.Makoshi, T.Mii, and H.Ueba, Surf. Sci. **493**, 63 (2001).

[10] T.Mii, S.Tikhodeev, and H.Ueba, Surf. Sci. **502-503**, 26 (2002).

[11] T.Mii, S.G.Tikhodeev, and H.Ueba, Phys. Rev. B **68**, 205406 (2003).

[12] M.Galperin, M.A.Ratner, and A.Nitzan, J. Chem. Phys. **121**, 11965 (2004).

[13] N.Lorente, M.Persson, L.-J.Lauhon, and W.Ho, Phys. Rev. Lett. **86**, 2593 (2001).

[14] M.-L.Bocquet, H.Lesnard, and N.Lorente Phys. Rev. Lett. **96**, 096101 (2006).

[15] T.Frederiksen, M.Brandbyge, N.Lorente, and A.-P.Jauho, Phys. Rev. Lett. **93**, 256601 (2004).

[16] M.Paulsson, T.Frederiksen and M.Brandbyge, Nano Lett. **6**, 258 (2006)

[17] N.Lorente and M.Persson, Phys. Rev. Lett. **85**, 2997 (2000)

[18] A.Pecchia, A. Di Carlo, A.Gagliardi, S.Sanna, T.Frauenheim, and R.Gutierrez, Nano Lett. **4**, 2109 (2004).

[19] P.Hyldgaard, S.Hershfield, J.H.Davies, and J.W.Wilkins, Ann. Phys. **236**, 1 (1994).

[20] A.Mitra, I.Aleiner, and A.J.Millis, Phys. Rev. B **69**, 245302 (2004).

[21] N.S.Wingreen, K.W.Jacobsen, and J.W.Wilkins, Phys. Rev. Lett. **61**, 1396 (1988).

[22] N.S.Wingreen, K.W.Jacobsen, and J.W.Wilkins, Phys. Rev. B **40**, 11834 (1989).

[23] J.Bonča and S.A.Trugman, Phys. Rev. Lett. **75**, 2566 (1995).

[24] A.S.Alexandrov and A.M.Bratkovsky, Phys. Rev. B **67**, 235312 (2003).

[25] B.Muralidharan, A.W.Ghosh, and S.Datta, Phys. Rev. B **73**, 155410 (2006).

[26] L.Siddiqui, A.W.Ghosh, and S.Datta, Phys. Rev. B **76**, 085433 (2007).

[27] K.Flensberg, Phys. Rev. B **68**, 205323 (2003).

[28] M.Galperin, A.Nitzan, and M.A.Ratner, Phys. Rev. B **73**, 045314 (2006).

[29] R.Härtle, C.Benesch, and M.Thoss, arXiv:0801.3602 (2008).

[30] M.Galperin, M.A.Ratner, and A. Nitzan, Nano Lett. **5**, 125 (2005); J. Phys.: Condens. Matter to be published (2008).

[31] A. La Magna and I.Deretzis, Phys. Rev. Lett. **99**, 136404 (2007).

[32] A.M.Kuznetsov, J. Chem. Phys. **127**, 084710 (2007).

[33] A.Mitra, I.Aleiner, and A.J.Millis, Phys. Rev. Lett. **94**, 076404 (2005).

[34] D.Mozyrsky, M.B.Hastings, and I.Martin, Phys. Rev. B **73**, 035104 (2006).

[35] J.P.Bergfield and C.A.Stafford, arXiv:0803.2756 (2008).

[36] H.Schoeller, Lecture Notes in Physics **544**, 137 (2000).

[37] J.Rammer, A.L.Shelankov, and J.Wabnig, Phys. Rev. B **70**, 115327 (2004).

[38] I.Sandalov, J.Johansson, and O.Eriksson, Int. J. Quant. Chem. **94**, 113 (2003).

[39] J.Fransson, O.Eriksson, and I.Sandalov, Phys. Rev. Lett. **88**, 226601 (2002).

[40] J.Fransson, Phys. Rev. B **72**, 075314 (2005).

[41] I.Sandalov and R.G.Nazmitdinov, Phys. Rev. B **75**, 075315 (2007).

[42] J.Fransson, O.Eriksson, and I.Sandalov, Photonics and Nanostructures **2**, 11 (2004).

[43] J.Fransson and O.Eriksson, J. Phys.: Condens. Matter **16**, L85 (2004).

[44] J.Fransson, Phys. Rev. B **69**, 201304(R) (2004).

[45] J.Fransson and O.Eriksson, Phys. Rev. B **70**, 085301 (2004).

[46] M.Galperin, A.Nitzan, and M.A.Ratner, Phys. Rev. B **74**, 075326 (2006).

[47] T.S.Rahman, R.S.Knox, and V.M.Kenkre, Chem. Phys. **44**, 197 (1979).

[48] J.Fransson, O.Eriksson, and I.Sandalov, Phys. Rev. B **66**, 195319 (2002).

[49] Y.Meir and N.S.Wingreen, Phys. Rev. Lett. **68**, 2512 (1992).

[50] H.Haug and A.Jauho, *Quantum Kinetics in Transport and Optics of Semiconductors* Springer-Verlag: Berlin, Heidelberg (1996).

[51] M.Galperin, A.Nitzan, and M.A.Ratner, Phys. Rev. B **76**, 035301 (2007).

[52] G.D.Mahan, *Many-Particle Physics*, Kluwer Academic/Plenum Publishers: New York (2000).

[53] P.T.Ruhoff, Chem. Phys. **186**, 355 (1994).

[54] P.T.Ruhoff and M.A.Ratner, Int. J. Quant. Chem. **77**, 383 (2000).

[55] R.Bulla, T.A.Costi, and T.Pruschke, Rev. Mod. Phys. **80**, 395 (2008).

[56] K.A.Al-Hassanieh, A.E.Feiguin, J.A.Riera, C.A.Busser, and E.Dagotto, Phys. Rev. B **73**, 195304 (2006).

[57] J.E.Han, Phys. Rev. B **73**, 125319 (2006).

[58] P.S.Cornaglia, G.Usaj, and C.A.Balseiro, Phys. Rev. B **76**, 241403(R) (2007).

[59] F.B.Anders, Phys. Rev. Lett. **101**, 066804 (2008).

[60] Note, that approximation like the one presented in Section II D may result in unphysical behavior. In particular, retarded and advanced SEs and GFs are not Hermitian conjugates of one another. While the issue does not arise in the diagonal approximation implemented for calculations here, this is a problem for a more general consideration. A simple workaround is to use average of two Dyson-like expressions: one with $\hat{D}^{-1}$, Eq.(35), applied from the left and one from the right. This leads to set of equations for GFs, which under Markov approximation reduce to widely employed equations for DM in dissipative environment.